

# **Effects of Stents under Asymmetric Inflow Conditions**

M.A. Atherton\*, K. Tesch & M.W. Collins, South Bank University, London, UK

#### **Abstract**

Patient-to-patient variations in artery geometry may determine their susceptibility to stenosis formation. These geometrical variations can be linked to variations in flow characteristics such as wall shear stress through stents, which increases the risk of restenosis. This paper considers computer models of stents in non-symmetric flows and their effects on flow characteristics at the wall. This is a fresh approach from the point of view of identifying a stent design whose performance is insensitive to asymmetric flow. Measures of dissipated energy and power are introduced in order to discriminate between competing designs of stents.

## 1. Introduction

Cardiovascular stents (Fig. 1) are mechanical devices for dilating arteries in order to relieve blockages or *stenoses*. Dilation is secured using an angioplasty balloon that expands the stent beyond its elastic limit at the site of a lesion. The use of stents has been a standard clinical treatment since 1987 [6] and yet re-stenosis occurs in 20%-40% of cases [13]. Just a small reduction in this figure offers enormous potential savings in cost [1]. The characteristics of fluid flow, such as wall shear stress, have been identified as a major contributory factor [4]. Coronary artery stents have been shown to induce flow disturbances [7], which significantly increases wall shear stress contributing to restenosis because it delays endothelial cell growth.



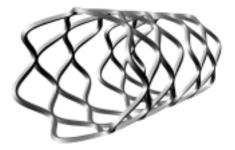


Figure 1. Stent models based on Guidant Multilink and Palmaz-Schatz PS 153 designs.

Patient-to-patient variation in the geometry of arterial bifurcations and its effect on flow conditions has received significant attention [2,3,5,12]; and has been described as the 'geometric risk factor'. Furthermore it has been suggested that geometric variations may be

E: mark.atherton@sbu.ac.uk T: +44 (0) 20 7815 7679 F: +44 (0) 20 7815 7699

\_

<sup>\*</sup>Dr Mark Atherton, BioMedical Engineering & Design Research Group, School of Engineering, South Bank University, Borough Road, London, SE1 0AA

responsible for the variability in susceptibility to atherosclerosis (thickening of arteries) and stenosis formation from one individual to another. Therefore restenosis can be linked to asymmetry in terms of variations of artery geometry, flow behaviour and stent-artery wall contact.

Intuitively, a purely axial inflow would promote stent patterns symmetric about the axis and so our longer-term aim is to investigate the influence of non-axial (asymmetric) flows on stent design. The inflow conditions in a design context are thus termed 'noise factors' and are akin to the geometric risk factor, as a good stent design should be insensitive to a range of such noise conditions in vivo. In this paper the effects of stent design on flow characteristics under such asymmetric conditions is explored. Designs based on the Palmaz-Schatz PS 153 (PS) and the Guidant Multilink (GM) are considered, which represent two of the most successful stents in use [9] and share the same basic pattern elements. The PS stent pattern is made up of corrugated rings mirrored to join at the peaks. The GM stent pattern repeats the corrugated rings and therefore requires joining links.

### 2. Method

A typical 3mm artery was the subject, rather than carotid or coronary arteries specifically, on the recommendation of our clinical collaborator [10]. As a first approximation, Computational Fluid Dynamics simulations employed full 3D rigid models of stents placed in idealised straight cylindrical arteries with inflow determined by straight or curved (9mm radius) entry tubes. By curved we mean in one plane, however the method could be extended to accommodate 'twisting', which is a type of flow that could also be expected. This provided a simple representation of the combined effects of variation in artery geometry and flow conditions (e.g. swirling flow). Thus the 'noise factor' was straight or curved flow entry. Unsteady state results were obtained over a complete pulse cycle (Fig. 2).

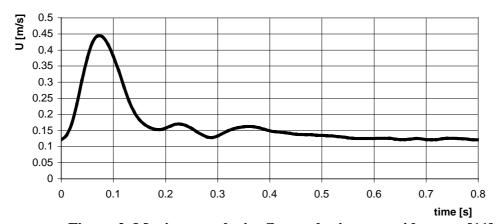


Figure 2. Maximum velocity flow pulse in a carotid artery [11].

As a means of overcoming hardware/software meshing limitations 'partial models' of stent sub-regions were developed, enabling the representation of linking elements between stent rings for square strut sections. These stent models were subject to steady state inlet flow with

angles between 0 degrees and 45 degrees (Fig. 3b) to the stent axis, representing a 'noise factor'. The velocity field caused by the single-plane curved entry was correctly incorporated.

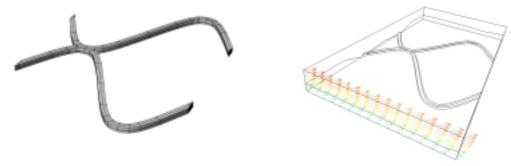


Figure 3. (a) PS stent partial model

(b) Inlet velocity profile.

For full 3D stents, integrating mean and standard deviation of wall shear stress values over the pulse cycle for all wall nodes provided performance measures. In addition, measures of dissipated energy (Equation 1) and dissipated power (Equation 2) were developed for quantifying stent performance with full and partial models respectively.

Firstly, dissipated power for an incompressible fluid:

$$N_{diss} := \iiint_{V} \mathbf{P} : \nabla \vec{\mathbf{U}} dx dy dz \tag{1}$$

Where:  $\vec{U}$  is the velocity vector field. P is a stress tensor, V is the volume of the flow domain.

The constitutive equation of **P**, describing the relationship between the stress tensor and shear strain rate tensor, is  $\mathbf{P} = -p\mathbf{E} + 2\mu\mathbf{D}$ . **E** is an identity tensor and **D** the shear strain rate

tensor given by 
$$\mathbf{D} := \frac{1}{2} \left[ \frac{\partial U_i}{\partial x_j} + \frac{\partial U_j}{\partial x_i} \right].$$

For a non-Newtonian fluid, the dynamic viscosity may be written according to a power law

$$\mu = k(2\mathbf{D} : \mathbf{D})^{\frac{n-1}{2}}$$
, where k and n are constant, e.g. for blood  $n = 0.61$ ,  $k = 0.042$  [kg m<sup>-1</sup> s<sup>-1.39</sup>].

Thus in order to calculate dissipated power only the velocity field is needed. The velocity field is obtained from numerical solution of the Navier–Stokes equations for incompressible flow. Dissipated energy is more accurate for transient calculations  $E_{\text{diss}} := \int\limits_t^t N_{\text{diss}} dt$ , where t is

the pulse cycle duration.

$$E_{diss} := \int_{t} dt \iiint_{V} \mathbf{P} : \nabla \vec{\mathbf{U}} dx dy dz$$
 (2)

After evaluating stent performance with the full 3D models using Equation 2 over the complete flow pulse cycle, it was deemed sufficient for comparison purposes to use the partial models and Equation 1 at maximum flow velocity. The validity of the algorithms for Equation 1 and Equation 2 was checked for different types of elements by comparing the results with the analytical solutions for dissipation of flow in a cylinder.

# 3. Results

In this investigation the flow asymmetry was in one plane only. Therefore while the full model was resolved according to the maximum storage available, it was also possible to use a partial model to get more detailed information (Fig. 4). We carried out a model/mesh refinement exercise and this confirmed that stent-to-stent comparisons of averaged Wall Shear Stress were sufficiently similar for both full and partial models for design purposes (12.2% and 10.7% respectively for the least and most refined cases). Validity was also checked by comparing computed values of dissipated power with analytical solutions for the case of an artery with no stent (maximum of 4% difference). Finally, convergence was fully achieved for all numerical solutions within a residual of 1e-04.

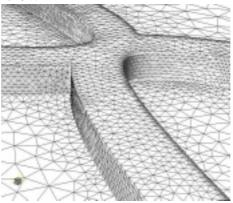


Figure 4. Element mesh for partial models.

The results of calculating wall shear stress (WSS) and dissipated energy for the full models are summarised in Table 1. It should be noted that dissipated energy is a dissipated power value integrated over time in accordance with Equation 2. The WSS values were integrated over time from values averaged over each time step then the result was divided by the pulse cycle duration to yield the time-averaged mean and standard deviation of WSS.

	1	0,		8	
Stent design	Flow entry	tube	Dissipated Energy [J]	Time-averaged mean WSS [N/m²]	Time-averaged standard deviation WS

Table 1. Dissipated energy for full models of stent designs under two inflow conditions

Stent design	riow entry tube	Dissipated Energy [J]	mean WSS [N/m <sup>2</sup> ]	standard deviation WSS [N/m²]
No stent	straight	0.0063	0.0266	0.0055
No stent	curved	0.0102	0.0318	0.0103
PS	straight	0.0086	0.0413	0.0409
PS	curved	0.0128	0.0416	0.0413
'GMr'	straight	0.0076	0.0395	0.0364
'GMr'	curved	0.0117	0.0400	0.0366

The stent wire cross sections of PS and GM stents are both square sections. However, in Table 1, 'GMr' is a stent design with the basic pattern of a Guidant Multilink but with a rounded strut section. Results of calculating dissipated power for the partial models are summarised in Table 2.

Table 2. Dissipated power for partial models of stent designs under several angles of inflow

	Dissipated Power [W]							
Stent design	0 degree inlet	15 degree inlet	30 degree inlet	45 degree inlet				
PS	3.07E-06	3.07E-06	3.09E-06	3.14E-06				
'PSr'	2.62E-06	2.63E-06	2.64E-06	2.67E-06				
GM	3.24E-06	3.23E-06	3.25E-06	3.32E-06				
'GMr'	2.70E-06	2.70E-06	2.71E-06	2.76E-06				
'GMnl'	3.19E-06	3.19E-06	3.20E-06	3.26E-06				

'PSr' is a stent design with the basic pattern of a Palmaz-Schatz but with a rounded section. 'GMr' is the same design as in Table 1. 'GMnl' is a stent design with the basic pattern of a Guidant Multilink but without the (necessary) linking members between rings. Table 2 is presented graphically in Figure 5.

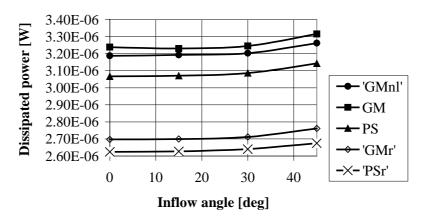


Figure 5: Plots of dissipated power for stent designs under several angles of inlet flow.

### 4. Discussion and Conclusions

In this paper our motive has been to obtain results that while justifiable in terms of CFD provides tools for design decisions. Our approach is consistent with recent clinical interpretations of stent versus stent comparisons [8].

From Table 1, it can be seen that dissipated energy is a more discriminating measure of the effects on flow characteristics of curved inflow conditions than time-averaged wall shear stress values. The effect of artery curvature (asymmetry) on flow performance is considerable, for example, for no stent conditions mean wall shear stress value in the artery increases 19% and dissipated energy increases 62%. With stents, the dissipated energy increases 50%. The effects of stent design are interesting as the 'GMr' stent design is clearly less disruptive to the flow than the PS stent both in terms of mean WSS (>4% lower) and dissipated energy (>10% lower).

Recalling that WSS is a characteristic thought to be significant in restenosis, it is interesting that WSS is a measure of work expended against wall friction, by this we mean friction with the stent surface and the endothelial surface. This also relates to dissipated energy, which is

rather similar to friction factor in heat exchangers in that it is a measure related to pressure drop.

Table 2 highlights the effects on performance of design details, most notably the 15% reduction in dissipated power when using a rounded strut section. Designs such as 'GMnl' do not necessarily represent viable solutions but the results serve to highlight the effects of links on GM design performance. Moreover, amongst these partial models, PS and 'GMnl' designs only differ in respect of the phase shift between the two rings yet exhibit 4% performance difference. The effect of a 45-degree inlet flow angle (2%) for steady state conditions is much less than the effect of curvature for unsteady state inflow conditions above.

The relative importance of features such as, pattern, strut section and links will be explored in future. Geometric risk factors will be addressed in greater detail, in terms of artery shape and degree of stent embedding. The results indicate that, on the limited rationale of these performance measures only, the stent design can contribute to restenosis. We conclude that the inflow conditions are sufficiently significant noise factors for the stent to have wide latitude with regards to inflow angle, which equates to a low flat curve in Fig. 5.

#### References

- [1] G.I. Frank, Basic considerations for coronary stenting, in: *Coronary Stents*, U. Sigwart and G.I. Frank, eds, Springer-Verlag, 1992, p5.
- [2] M.H. Friedman, O.J. Deters, F.F. Mark, C.B. Bargeron, and G.M. Hutchins, Arterial geometry affects hemodynamics. *Atherosclerosis*, **46**, (1983), 225-231.
- [3] M.H. Friedman, P.B. Baker, Z. Ding, and B.D. Kuban, Relationship between the geometry and quantitative morphology of the left anterior descending coronary artery. *Atherosclerosis*, **125**, (1996), 183-192.
- [4] A.H Goodhall, Role of shear stress and turbulence on platelets in blood conduits and on endothelial cells in arterial conduits, in: *Endoluminal Stenting*, U. Sigwart, ed, 1996, pp. 65-78.
- [5] R.M. Nerem, and M.J. Levesque, The case for fluid dynamics as a localising factor in atherogenesis, in: *Fluid Dynamics as a Localizing Factor for Atherosclerosis*, G. Schettler, R.M. Nerem, H Schmid-Schönbein, H. Mörl and C. Deim, eds, Springer, Berlin-Heidelberg-New York, 1983, pp 26-37.
- [6] S.N. Osterle et al, The stent decade: 1987 to 1997, American Heart Journal. 136:4/1 (1998), 578-599.
- [7] J. Peacock, S. Hankins, T. Jones and R. Lutz, Flow instabilities induced by coronary artery stents: assessment with an *in vitro* pulse duplicator, *J. Biomechanics*. **28:1** (1995), 17-26.
- [8] J.J. Popma, Stent selection in clinical practice: Have clinical trials provided the evidence we need?, *American Heart Journal.* **142:3** (2001), 378-380.
- [9] P.W. Serruys and M.J.B. Kutryk, eds, *Handbook of Coronary Stents*, Martin Duntiz Ltd, 1998.
- [10] U. Sigwart, Consultant Cardiologist, Royal Brompton Hospital, London. Personal communication.
- [11] D.A. Steinman, B. Vinh, C.R. Ethier, M. Ojha, R.S.C. Cobbold, and K.W. Johnston, A numerical simulation of flow in a two-dimensional end-to-side anastomosis model, *ASME J. Biomechanical Eng.*, **115**, (1993), 112-118.
- [12] H.Sun, B.D. Kuban, P. Schmalbrock, and M.H. Friedman, Measurement of the geometric parameters of the aortic bifurcation from magnetic resonance images. *Annals of Biomedical Engineering*, **22**, (1994), 229-239.
- [13] H.J.C. Swan, Coronary Stents Introduction, in: *Coronary Stents*, U. Sigwart and G.I. Frank, eds, Springer-Verlag, 1992, p1.